

David Anssari Moin  
Bassam Hassan  
Azin Parsa  
Peter Mercelis  
Daniel Wismeijer

# Accuracy of preemptively constructed, Cone Beam CT-, and CAD/CAM technology-based, individual Root Analogue Implant technique: An *in vitro* pilot investigation

## Authors' affiliations:

David Anssari Moin, Bassam Hassan, Daniel Wismeijer, Department of Oral Function and Restorative Dentistry, Academic Centre for Dentistry Amsterdam (ACTA), Research Institute Move, Amsterdam, The Netherlands  
Azin Parsa, Department of Radiology, Academic Centre for Dentistry Amsterdam (ACTA), Amsterdam, The Netherlands  
Peter Mercelis, DentWise division, LayerWise NV, Leuven, Belgium

## Corresponding author:

David Anssari Moin, MSc  
Department of Oral Function  
Academic Centre for Dentistry Amsterdam (ACTA)  
Gustav Mahlerlaan 3004  
1081 LA Amsterdam, The Netherlands  
Tel.: + (31) (0)20-5980322  
e-mail: danssari@acta.nl

**Key words:** biomaterials, biomechanics, CT imaging, finite element analysis, imaging, material sciences, radiology

## Abstract

**Objectives:** The aim of this *in vitro* pilot investigation is to assess the accuracy of the preemptive individually fabricated root analogue implant (RAI) based on three-dimensional (3D) root surface models obtained from a cone beam computed tomography (CBCT) scan, computer-aided designing (CAD), and computer-aided manufacturing (CAM) technology and to measure the discrepancy in congruence with the alveolar socket subsequent to placement of the RAI.

**Materials and methods:** Eleven single-rooted teeth from nine human cadaver mandibles were scanned with the 3D Accuitomo 170 CBCT system. The 3D surface reconstructions of the teeth acquired from the CBCT scans were used as input for fabrication of the RAIs in titanium using rapid manufacturing technology. The teeth were then carefully extracted. The teeth and RAIs were consequently optically scanned. The mandibles with the empty extraction sockets were scanned with CBCT using identical settings to the first scan. Finally, the preemptively made RAIs were implanted into their respective sockets, and the mandibles were again scanned with CBCT using the same scan settings as previous scans. All 3D surface reconstructions (CBCT 3D surface models and optical scan 3D models) were saved for further analysis. 3D models of original teeth and optical scans of the RAIs were superimposed onto each other; differences were quantified as root mean square (RMS) and Hausdorff surface distance. To obtain an estimate of the fit (congruence) of the RAIs in their respective sockets, the volumetric data sets of the sockets were compared with those of the root part of RAIs congruent with the sockets.

**Results:** Superimposed surfaces of the RAIs and the original tooth reveal discrepancy for RMS, volumetric geometry, and surface area varying from 0.08 mm to 0.35 mm, 0.1% to 7.9%, and 1.1% to 3.8%, respectively. Comparing volume differences of the alveolus with the socket corresponding part of the RAI resulted in every case the volume of the socket being greater than the root part of the RAI ranging from 0.6% to 5.9% volume difference.

**Conclusion:** The preemptive CAD/CAM-based RAI technique might offer promising features for immediate implant placement. However, due to the lack of prospective clinical data, further research is needed to fine-tune and evaluate this technique.

The use of cone beam computed tomography (CBCT), computer-aided designing (CAD), and computer-aided manufacturing (CAM) has become widespread in implant dentistry. Various clinical applications including computerized implant treatment planning, implant-supported fixed prosthesis, and guided implant surgery combine the use of CBCT and CAD/CAM technologies (Jung et al. 2009). As technology advances, applications of digitized dental reconstructions will continue to expand.

Recently, we proposed a novel approach for immediate implant placement designed to replace a (soon to be) missing tooth (Anssari Moin et al. 2011). In contrast to traditional immediate implant approaches using conventional, threaded, cylindrical, or tapered implants, this technique provides a preemptively individually made root analogue implant (RAI) based on acquisition of three-dimensional (3D) reconstructions from the CBCT scan and fabrication process through

## Date:

Accepted 10 November 2012

## To cite this article:

Anssari Moin D, Hassan B, Parsa A, Mercelis P, Wismeijer D. Accuracy of preemptively constructed, Cone Beam CT-, and CAD/CAM technology-based, individual Root Analogue Implant technique: an *in vitro* pilot investigation. *Clin. Oral Impl. Res.* 00, 2012, 1–5  
doi: 10.1111/clr.12104

high-end selective laser melting (SLM) technology.

Our pilot study results suggested that the dimensions of the RAI are similar to the original root. However, all steps in the process of fabricating a preemptively made RAI can result in geometrical deviations and structural imperfections. Consequently, these errors can lead to discrepancies in implant fit in the socket, lessened bone-to-implant contact, decreased mechanical engagement of the implant, or highly pressurized implant fit. For successful implementation of the preemptive RAI technique, high-quality 3D surface models, high-accuracy fabrication of the RAI, and a congruent fit between the RAI and the extraction socket are required (Anssari Moin et al. 2011; Figliuzzi et al. 2012). The aim of this pilot investigation is to assess the accuracy of the individually fabricated CBCT- and CAD/CAM-based titanium RAI and to measure the discrepancy in congruence with the alveolar socket subsequent to placement.

## Materials and methods

### Sample preparation, radiographic scan, optical scan, and CAD/CAM process

We built on the method previously described by Anssari Moin et al. 2011; . Briefly, eleven single-rooted teeth from nine mandibles (not identified by age, gender, or ethnic group) were selected. There were three central and one lateral incisor and six canines and one premolar tooth. The mandibles were scanned with the 3D Accuitomo 170 CBCT system (Accuitomo 170, 90kVp, 5 mA, 30.8 s, 4 x 4 cm Field of View [FoV], voxel 0.08 mm<sup>3</sup>, Morita Inc., Kyoto, Japan) using the recommended scan protocol. Subsequently, eleven RAIs were produced in titanium by rapid manufacturing using SLM technology (LayerWise NV, Dent-Wise Division, Leuven, Belgium). The 3D surface reconstructions of the teeth acquired from the CBCT scans were used as the input for the digital manufacturing process (3D

reconstruction details follow below). The files were sliced with a layer thickness of 30 µm and produced in a high-end SLM machine equipped with an ytterbium fiber laser from Ti6Al4V powder under an argon atmosphere.

The teeth were then carefully extracted to reduce risk of fracturing the bone and roots and to avoid any alterations to the shape of the socket. The teeth and RAIs were consequently optically scanned using an optical system (Atos II SO; GOM GmbH, Braunschweig, Germany). Subsequent to tooth extraction and prior to RAI implantation, the mandibles with the empty extraction sockets were scanned with CBCT using identical settings to the first scan. This was conducted to obtain the volumes of the sockets after extraction.

Finally, the preemptively made RAIs were implanted into their respective sockets. With finger pressure and the gentle use of a hammer and a mallet, good primary stability of the RAI was achieved and checked by palpation and percussion. The nine mandibles with the eleven RAIs in place were again scanned with the 3D Accuitomo 170 CBCT system using the exact same scan settings as with the previous scans.

### 3D surface reconstructions, surface measurements, and volumetric measurements

The CBCT data sets were imported in Amira software for further analysis and image segmentation (v 5.3, Visage Imaging, Carlsbad, CA, USA). Threshold-based segmentation techniques were employed to segment the teeth from their surroundings in the original scan prior to tooth extraction (Fig. 1). The exact procedure for segmenting the tooth was the following: A region of interest limited to the tooth and surrounding periodontium was first selected. Subsequently, an optimal threshold value based on the histogram analysis, the local gray level value, and image gradient was selected to separate the root and crown from the surrounding bone. A manual selection, on the basis of the sagittal slides, was added for

the most apical part of the root if the threshold-based technique did not confine the entire apex area. The resulting images were processed using interactive processing tools to remove resulting artifacts.

All segmented data sets were converted to 3D surface models using the marching cube algorithm (Lorensen & Cline 1987). The 3D surfaces were saved in the standardized triangulation language (STL) file format. The same format was employed for the optical 3D models of the natural teeth and RAIs (Fig. 2 a, b). Using a 3D iterative closest point registration algorithm (Aloimonos 2004), 3D models of the teeth and the optical scans of the RAIs were superimposed onto each other, and differences were quantified as mean (root mean square [RMS]) and maximum (hausdorff) surface distance (Canadian Image Processing Pattern Recognition Society 2004) (Fig. 2c). The STL of the natural tooth served as the reference standard within alignment of the surfaces.

To obtain an estimate of the fit (congruence) of the RAIs in their respective sockets, the volumetric data sets of the sockets were compared with the volumetric data sets of the root part of RAIs congruent with the sockets. The measurement process was as follows: Using tracing tools in Amira, the outline of the socket was followed on each slice starting coronally at the alveolar bone crest and proceeding apically to the apex. On each slice, a contour was traced and the confined surface area was automatically selected through the software (Fig. 3).

The volumes were obtained through combining the surface areas of the contiguous slices and considering the voxel dimensions. The software then automatically measures the sum total of the volumes of the individual slices producing the total volume of the socket in cubic millimeter. This method has been previously described to follow up volumetric bone or soft tissue changes with CBCT (Garcia de Paula-Silva et al. 2009). The same volumetric measurement process was applied for to the alveolar socket corresponding part of the implanted RAI.

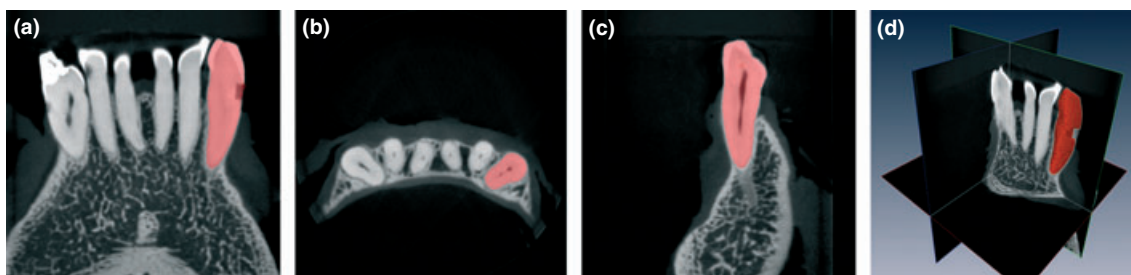


Fig. 1. Example of the segmentation and preparation of RAI no. 2. Coronal (a), axial (b), sagittal (c), and 3D (d) views.

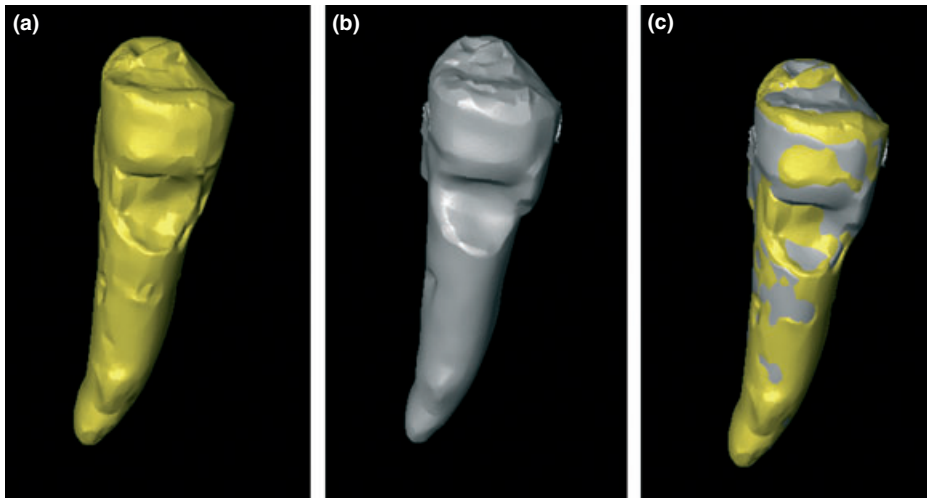


Fig. 2. 3D surface models derived from optical scanning of the natural tooth (a) and from optical scanning of the RAI (b). Surface alignment between natural tooth (yellow) and RAI (gray) in (c). Notice the under-estimation of RAI surface reconstruction in comparison with the natural tooth, especially in the apical area.

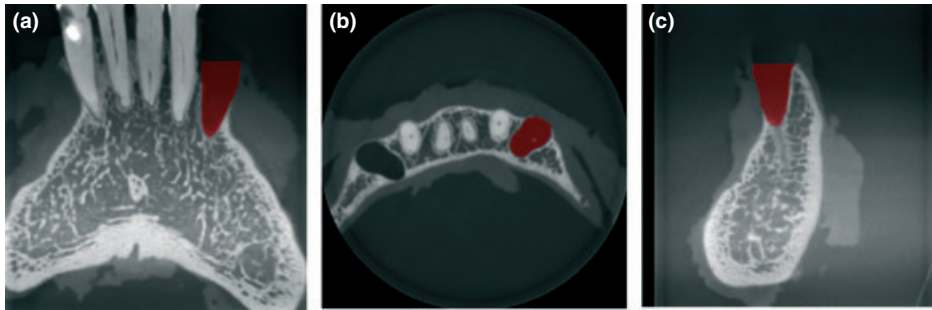


Fig. 3. Example of the volumetric measurement of the socket of RAI no. 2. Coronal (a), axial (b), and sagittal (c) views.

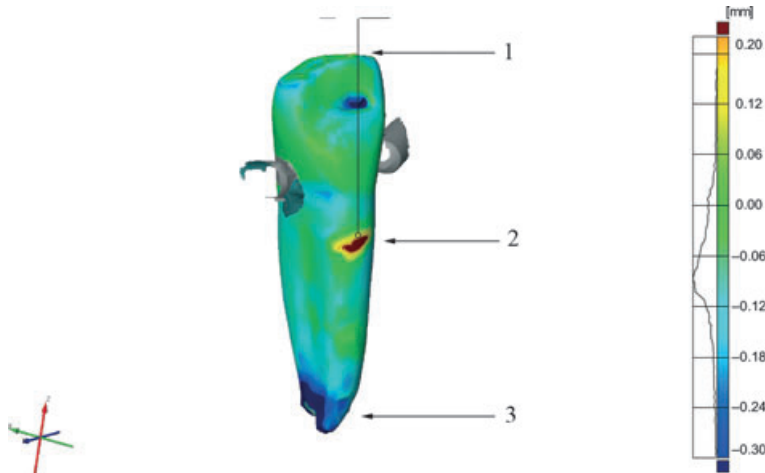


Fig. 4. Superimposed STL files of the optical scan of the original tooth and RAI no. 2. Measurement in millimeters. Notice: optical scan of the tooth served as the reference surface.

Results

Comparing the superimposed surfaces of the RAIs and the original tooth reveals in all eleven cases a local disparity at the incisal

edge area (Fig. 4, arrow 1). This particular incisal edge area of the RAIs is smaller than the original teeth (maximum 0.15 mm). Toward the more apical areas, all RAIs appear to have gradual deviation with their

original counterparts (Fig. 4, arrow 3) varying with a minimum of 0.31 mm and a maximum of 1.86 mm decrease at the most apical part of the RAIs. At the cemento-enamel junction (CEJ) of RAI nos. 2, 4, 5, 6, 7, 8, and 9, a local increase in surface area is visible (Fig. 4, arrow 2).

The RMS data, volume change, and surface area change between the RAI and original tooth were measured for all RAIs (summarized in Table 1, column A, B, and C. Note: the natural tooth served as reference). The RAIs were smaller than the original teeth in all instances (Fig. 2 c). The discrepancy for the RMS, volumetric geometry, and surface area varied from 0.08 mm to 0.35 mm, 0.1% to 7.9%, and 1.1% to 3.8%, respectively.

To ascertain the extent of congruence of the root part of the RAIs with their equivalent sockets, volume differences of the alveolus with the socket corresponding part of the RAI were calculated (outlined in Table 1, column D. Note: the empty socket served as reference). In every case, the volume of the socket was greater than the root part of the RAI ranging from 0.6% to 5.9% volume difference.

Discussion

Advantages supporting the idea of this approach encompass shortening of the reconstruction treatment time, forbearance of multiple surgical interventions, and easy surgical handling, altogether resulting in increased patient comfort. Another proposed advantage of the technique is the minimal marginal alveolar bone resorption as a consequence of the uncomplicated surgical application: atraumatic, flap-less, and socket friendly (Pirker et al. 2011; Figliuzzi et al. 2012). As the RAI is a one-piece and one-stage implant, submerged healing is not an option. Hence, after removal of the tooth and insertion of the RAI, primary stability is of crucial importance for osseointegration (Lioubavina-Hack et al. 2006). Conventional threaded implants achieve primary stability in immediate implantation situations by means of perforating 3–5 mm apically of the alveolus and screw retaining the implant into to the lingual/palatal alveolar bone wall (Lang et al. 2012). However, with the RAI, primary stability is achieved through a good congruence with the alveolar socket, a slight pressurized fit, and the macroscopic features of the implant (Pirker et al. 2011). It is of note that a pressurized fit is one of the key factors influencing primary stability. Inaccuracies from the digital planning to the

**Table 1. Summarized measurements: The natural tooth/socket served as reference standard**

	A RMS ± SD (max) Natural tooth vs. RAI	B Volume Natural tooth vs. RAI	C Surface area Natural tooth vs. RAI	D Volume socket Volume vs. RAI in socket
RAI 1	0.171 ± 0.122 (1.10)	2.5	1.1	0.6
RAI 2	0.155 ± 0.112 (1.11)	3.4	2.5	5.9
RAI 3	0.098 ± 0.070 (0.77)	3.6	3.8	1.4
RAI 4	0.119 ± 0.086 (1.87)	7.9	3.8	1.7
RAI 5	0.14 ± 0.095 (0.91)	2.2	2.3	2.5
RAI 6	0.14 ± 0.088 (1.01)	3.7	3.6	5.6
RAI 7	0.098 ± 0.067 (0.56)	2.2	1.3	1.7
RAI 8	0.35 ± 0.20 (1.06)	4.4	1.8	2.1
RAI 9	0.13 ± 0.095 (0.86)	0.1	1.4	3.1
RAI 10	0.080 ± 0.043 (0.31)	7.4	3.1	4.1
RAI 11	0.099 ± 0.061 (0.46)	6.0	1.7	1.7

Column A: RMS difference and standard deviation (SD) results between the optical scan of the natural tooth and the RAI in millimeters (mm). Maximum errors (Hausdorff distance) are reported between brackets. Column B: volume change (%) between the original tooth and fabricated RAI. Column C: surface area change (%) between the original tooth and RAI. Column D: volume difference (%) between the alveolar socket and implanted RAI.

fabrication process of the RAI will lead to decreased fit with the alveolar socket, lessened bone-to-implant contact, and abated primary stability and ultimately resulting in implant failure.

This pilot investigation was conducted to assess the accuracy of the preemptively constructed CBCT- and CAD/CAM-based RAI technique and measure for discrepancy with the socket after implantation. The results show that the differences between the RAI vs. tooth and socket vs. root part of the RAI are small. This is in corroboration with previous findings from Anssari Moin et al. 2011 and Figliuzzi et al. 2012; .

The particular disparity of the RAIs at the incisal edge can be rationalized by the fact that all the RAIs were supported with pins at the incisal edge during the SLM process. These supports were subsequently removed resulting in inaccuracy at this particular area. The gradual deviation increase in apical direction between the RAI and original tooth has previously been reported to be a cause of increased bone mass in apical direction resulting in lesser accuracy and gradual underestimation of the root during the segmentation process (Anssari Moin et al. 2011). Furthermore, the local incongruity of RAI nos. 2, 4, 5, 6, 7, 8, and 9 at the CEJ could be explained as damage to

the original tooth caused by extraction by forceps (Anssari Moin et al. 2011).

The study by Figliuzzi et al. 2012; is a clinical case report of the RAI. As it was unknown what potential distortions or errors of deviation will result when using the preemptively fabricated RAI technique, they prepared three different RAIs with sequential percentage dimensional increments of 0%, 5%, and 10% of the same object. During surgery, the RAI with 0% volume increase was chosen to be implanted. In this pilot study, it has been shown that the volume of the root part of the RAI differs from 0.6% up to 5.9% with the socket. Consequently, it would be advisable when clinically applying the RAI to have preemptively prepared a RAI with 0% and 5.9% volume increase at the root section. Still, considering the limited amount of incongruence of the RAI with the original tooth and the socket, it is not known whether these differences will be of clinical significance. Furthermore, it should be taken into consideration when (digitally) adding macro-retention to the RAI, volume increase of the RAI might not be of beneficial effect on primary stability (Pirker et al. 2011).

An important drawback of this proof of principle study is the use of cadavers. The

voxel size employed in this investigation of 0.08 mm might not be achievable in the clinic because real patients' scans suffer from motion artifacts related to slight patient's movement plus artifacts, resulting from the presence of anatomic structures outside the center of field of view (Schulze et al. 2011). These artifacts negatively contribute to the quality of the obtained images, so that effective system resolution would be lower (0.3–0.5 mm) than the nominal resolution of 0.08 mm reported here (Kalender & Kyriakou 2007). Different CBCT systems and scan settings would also influence the quality of the 3D model reconstructions (Loubele et al. 2007; Hassan et al. 2010a,b). Additionally, parameters of the SLM technique (Ti6Al4V alloy particle size, wave length, power, scanning rate, and laser spot size) will have consequences in the final results of the RAI. However, in this investigation, accuracy of the SLM technique was very high. Mean variation was from 0.015 mm to 0.020 mm when comparing the STL with the fabricated RAI.

Restoration of the RAI brings new digital challenges and potentials. Because the information of the RAI is in STL format, many alterations can be made to the RAI through computer 3D designing. Preoperatively designing the abutment form of the RAI in combination with 3D surface models of the dentition derived from CBCT might give the prospects of preemptively creating the (temporary) crown with CAD/CAM technology.

In conclusion, within the limitations of this *in vitro* investigation, it has been demonstrated that the preemptive CAD/CAM-based RAI technique could potentially provide accurate dental implants for immediate implant placement. However, the influence of the different image artifacts on segmentation accuracy could be investigated as the study sample was confined to human cadaver mandibles. Interesting possibilities arise when combining digital prosthetics and RAI technique. However, further clinical research is needed to fine-tune and evaluate this technique.

## References

- Aloimonos, J. (2004) IEEE Xplore 3DPVT 2nd International Symposium on 3D Data Processing, Visualization, and Transmission. Proceedings: 6–9 September, 2004, Thessaloniki, Greece University of Maryland, Institute for Advanced Computer Studies Institute of Electrical and Electronics Engineers Computer Society, Los Alamitos, California. **18**: 1014.
- Anssari Moin, D., Hassan, B., Mercelis, P. & Wismeijer, D. (2011) Designing a novel dental root analogue implant using cone beam computed tomography and CAD/CAM technology. *Clinical Oral Implants Research* doi: 10.1111/j.1600-0501.2011.02359.x.
- Canadian Image Processing Pattern Recognition Society. (2004) IEEE Xplore 1st Canadian Conference on Computer and Robot Vision. Proceedings: 17–19 May, 2004, Ontario, Canada. University of Western Ontario, International Association for Pattern Recognition. Institute of Electrical and Electronics Engineers Computer Society, Los Alamitos, California. **7**: 510.
- Figliuzzi, M., Mangano, F. & Mangano, C. (2012) A novel root analogue dental implant using CT scan and CAD/CAM: selective laser melting technology. *International Journal of Oral and Maxillofacial Surgery* **41**: 858–862.

- Garcia de Paula-Silva, F.W., Hassan, B., Bezerra da Silva, L.A., Leonardo, M.R. & Wu, M.K. (2009) Outcome of root canal treatment in dogs determined by periapical radiography and Cone-beam computed tomography scans. *Journal of Endodontology* **5**: 723–726.
- Hassan, B., Couto Souza, P., Jacobs, R., de Azambuja Berti, S. & van der Stelt, P. (2010b) Influence of scanning and reconstruction parameters on quality of three-dimensional surface models of the dental arches from cone beam computed tomography. *Clinical Oral Investigations* **14**: 303–310.
- Hassan, B., Metska, M.E., Ozok, A.R., van der Stelt, P. & Wesselink, P.R. (2010a) Comparison of five cone beam computed tomography systems for the detection of vertical root fractures. *Journal of Endodontology* **36**: 126–129.
- Jung, R.E., Schneider, D., Ganeles, J., Wismeijer, D., Zwahlen, M., Hammerle, C.H. & Tahmaseb, A. (2009) Computer technology applications in surgical implant dentistry: a systematic review. *International Journal of Oral and Maxillofacial Implants* **24**(Suppl): 92–109.
- Kalender, W.A. & Kyriakou, Y. (2007) Flat-detector computed tomography (FD-CT). *European Radiology* **17**: 2767–2779.
- Lang, N.P., Pun, L., Lau, K.Y., Li, K.Y. & Wong, M. C. (2012) A systematic review on survival and success rates of implants placed immediately into fresh extraction sockets after at least 1 year. *Clinical Oral Implants Research* **23**(Suppl 5): 39–66.
- Lioubavina-Hack, N., Lang, N.P. & Karring, T. (2006) Significance of primary stability for osseointegration of dental implants. *Clinical Oral Implants Research* **17**: 244–250.
- Lorensen, W.E. & Cline, H.E. (1987) Marching cubes: a high resolution 3D surface construction algorithm. *Association for Computing Machinery's Special Interest Group on Computer Graphics and Interactive Techniques* **21**: 163–169.
- Loubele, M., Guerrero, M.E., Jacobs, R., Suetens, P. & van Steenberghe, D. (2007) A comparison of jaw dimensional and quality assessments of bone characteristics with cone-beam CT, spiral tomography, and multi-slice spiral CT. *International Journal of Oral Maxillofacial Implants* **22**: 446–454.
- Pirker, W., Wiedemann, D., Lidauer, A. & Kocher, A.A. (2011) Immediate, single stage, truly anatomic zirconia implant in lower molar replacement: a case report with 2.5 years follow-up. *International Journal of Oral and Maxillofacial Surgery* **40**: 212–216.
- Schulze, R., Heil, U., Gross, D., Bruellmann, D.D., Dranischnikow, E., Schwanecke, U. & Schoemer, E. (2011) Artifacts in CBCT: a Review. *Dentomaxillofacial Radiology* **40**: 265–273.